Computational Fluid Dynamics Combustion Modeling for Rotating Detonation Engines

Peter A. Strakey[1a], Clinton R. Bedick[2b] and Donald H. Ferguson[3a]
U.S. Department of Energy
[a] *National Energy Technology Laboratory, Morgantown, WV 26507, USA*
[b] *National Energy Technology Laboratory, Pittsburgh, PA 15129, USA*

This paper focuses on the development and validation of a combustion model for Computational Fluid Dynamics (CFD) modeling of Rotating Detonation Engines. A zero-dimensional Partially Stirred Reactor (PaSR) with a detailed chemical kinetic mechanism for hydrogen and air is used to model turbulent combustion. The model is computationally efficient and is based on the notion of partial mixing at the sub-grid level with turbulent exchange between mixed and unmixed regions. The ability of the PaSR model to accurately represent both detonative and deflagrative combustion is assessed by validating the results against experimental data. The effects of mesh resolution on the solution are also studied in order to determine if a mesh independent solution is obtainable with the Large Eddy Simulation (LES) approach to modeling turbulence. A comparison is made between the PaSR model and simply ignoring turbulence chemistry interactions which assumes that all species are perfectly mixed at the sub-grid level.

I. Nomenclature

A	= area (m^2)
C_ε	= LES dynamic constant
c_p	= specific heat (J/kgK)
h^0	= enthalpy of formation (J/mol)
$\dot{m}$	= mass flow rate (kg/s)
M	= molecular weight (kg/mol)
P	= pressure (Pa)
T	= temperature (K)
V	= volume (m^3)
Y	= species mass fraction
Greek symbols	
Δ	= mesh size (m)
k	= turbulent kinetic energy (m^2/s^2)
ε	= turbulent dissipation rate (m^2/s^3)
κ	= PaSR model constant
φ	= equivalence ratio
ρ	= density (kg/m^3)
τ	= time scale (s)
ω	= source term (kg/s)
Subscripts	
e	= exit
i	= species index
mix	= mixing

[1] Research Scientist, Research and Innovation Center, AIAA member, peter.strakey@netl.doe.gov
[2] Research Scientist, Research and Innovation Center, AIAA member, clinton.bedick@netl.doe.gov
[3] Research Scientist, Research and Innovation Center, AIAA member, donald.ferguson@netl.doe.gov

0 = initial

Superscripts

* = reaction zone

0 = initial state

Acronyms

AFRL = Air Force Research Laboratory
BCD = Bounded Central Differencing
CFD = Computational Fluid Dynamics
CFL = Courant-Friedrichs-Lewy
CJ = Chapman-Jouget
DDT = Deflagration-to-Detonation Transition
EDC = Eddy Dissipation Concept
IR = InfraRed
LES = Large Eddy Simulation
NETL = National Energy Technology Laboratory
ODE = Ordinary Differential Equation
PaSR = Partially Stirred Reactor
PGC = Pressure Gain Combustion
RDE = Rotating Detonation Engine
SOU = Second Order Upwinding
UDF = User Defined Function

II. Introduction

Rotating detonation combustion is challenging to study and understand because of the extremely harsh environment including high frequency oscillations, supersonic speeds, high temperatures and pressures, and a small annulus area with varying modes of combustion occurring. As such, computational modeling of Rotating Detonation Engines (RDEs) has been a common approach to understanding the fundamental physics of these devices. One pronounced difficulty in modeling RDEs is the mixed modes of combustion involving both detonation and deflagration. The interaction of these combustion modes has a pronounced effect on detonation wave height, the number of waves, wave speed and overall performance. This paper focuses on the application of a combustion sub-model for Computational Fluid Dynamics (CFD) modeling of RDEs. To date, the vast majority of CFD studies of RDEs have not accounted for turbulence chemistry interactions and many don't include viscous effects at all [1, 2]. Ignoring turbulence chemistry interactions is analogous to assuming that scalars are perfectly mixed on the sub-grid scale. While this approach may work sufficiently well for detonation, the deflagrative burning that occurs is likely over predicted due to the lack of a combustion model.

There have been numerous combustion models developed for simulation of both turbulent premixed and non-premixed combustion [3, 4]. These models span the range of simplistic zero-dimensional models [5, 6] to multi-dimensional stochastic mixing models [7]. This study uses a Partially Stirred Reactor (PaSR) model [5-6, 8-9] which is based on the work of Byggstoyl and Magnussen [10] and similar in concept to the Eddy Dissipation Concept (EDC) model [11]. The PaSR model assumes that each computational cell is comprised of both reacting and non-reacting zones where mass is exchanged between the two through turbulent mixing. A conceptual drawing of the PaSR model for a single computational cell is shown in Fig. 1.

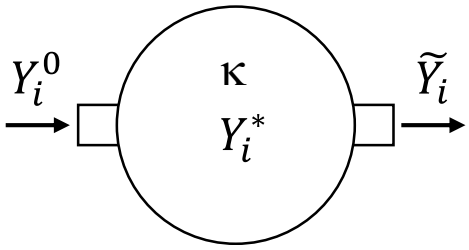

Fig. 1 Conceptual drawing of a single computational cell using the PaSR model.

The mean source terms for the species transport equations are expressed as:

$$\overline{\dot{\omega}_i} = \kappa \frac{\tilde{\rho}(Y_i^* - Y_i^0)}{\tau^*} \quad (1)$$

Where Y_i^0 is the initial ith species mass fraction in the non-reacting zone, Y_i^* is the ith species mass fraction in the reaction zone and $\widetilde{Y}_i$ is the final mean mass fraction of the ith species. The mean density is represented by $\tilde{\rho}$ and τ^* is the time spent in the reaction zone. The mass fraction of reacting mixture is calculated by the ratio of chemical to mixing timescales (Eq. (2)).

$$\kappa = \frac{\tau_c}{\tau_c + \tau_{mix}} \quad (2)$$

The simulations for this study were carried out with Ansys FLUENT 19.2 using an implicit pressure-based solver. An implicit method allows for a much larger time step compared to explicit density based approaches and was deemed to be a more practical for modeling full 3D RDE geometries with inlet manifolding. A Large Eddy Simulation (LES) turbulence model based on a transported turbulent kinetic energy equation was chosen with the turbulent mixing time being calculated as the ratio of turbulent kinetic energy to the dissipation rate ($\tau_{mix} = {}^{k}/_{\varepsilon}$), where ε is given by:

$$\varepsilon = C_\varepsilon \frac{k^{1.5}}{\Delta} \quad (3)$$

C_e is defined as a dynamically determined constant and Δ is the mesh cell size. There are many possible turbulent time scales to use and this approach represents a time scale based on the sub-grid integral turbulent scale. The chemical time scale is based on a normalized heat release rate [10] as shown in Eq. (4):

$$\tau_c = \frac{C_p(T - T_0)}{-\rho V \sum_i^I \frac{h_i^0}{M_i} \omega_i} \quad (4)$$

where C_p is the specific heat, T_0 is the unburned gas temperature, V is the cell volume, h_i^o is the heat of formation of species *i* and M_i is the molecular weight. Note that the species source terms, ω_i, are calculated prior to applying the PaSR constant κ.

The PaSR model is applicable to detailed, multi-step chemistry and the chemical model chosen here for hydrogen-air combustion is that of Li *et al.* [13] which is a 9-species, 19-step mechanism that has been validated across a wide range of pressures and temperatures. The PaSR model and detailed chemistry mechanism were implemented in Fluent through a User Defined Function (UDF). The chemistry was calculated with an operator splitting approach where the source terms are calculated using a stiff ODE solver at the beginning of each flow solver time step, then the turbulent and chemical time scales are calculated and the source terms are multiplied by κ (Eq. (2)).

III. Numerical Setup

The geometry studied here is an RDE design developed at the Air Force Research Laboratory (AFRL) [14] and adapted for use at the NETL high-pressure combustion facility. A schematic of the design is shown in Fig. 2 and incorporates a continuous air injection slot of 1.78 mm height with 120 discreet 0.89 mm diameter fuel injector holes. The annulus has an outer diameter of 154 mm and inner diameter of 139 mm and is 100 mm in length. While the experimental apparatus is capable of elevated back pressure, all of the simulation results presented here are for atmospheric pressure.

The hybrid mesh consisted of polyhedral cells in the inlet manifold and injector region with structured hexahedral cells in the annulus. A mesh sensitivity study was conducted by varying the nominal cell size from 1.5 to 0.25 mm in the detonation region of the annulus resulting in an overall cell counts ranging from 0.6 million to 29 million cells. The mesh size near the fuel injectors was typically about one fifth the nominal mesh size in the annulus. A contour plot of mesh cell size for the nominal 0.5 mm mesh with 6 million cells is shown in Fig. 3.

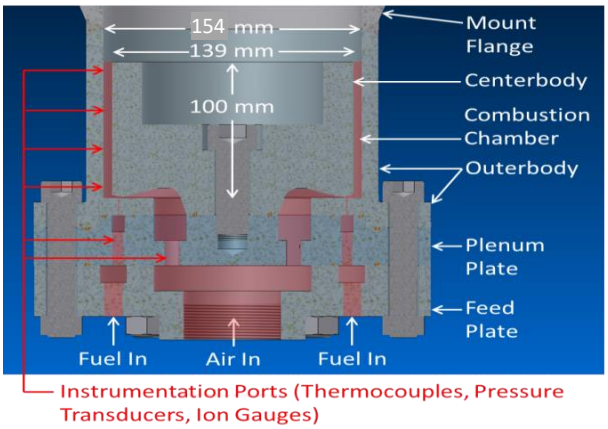

Fig. 2 Schematic of AFRL/NETL Rotating Detonation Engine.

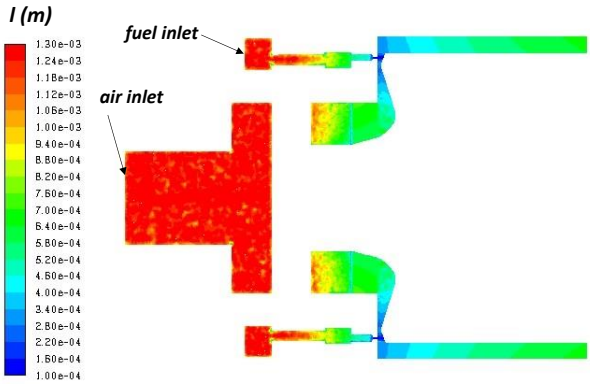

Fig. 3 Cross section of mesh size cutting through a fuel injector.

IV. Results and Discussion

A. 1-D Simulations

As pressure-based solvers are known to have difficulty in resolving discontinuities such as detonation waves, it is important to investigate the effect that numerical discretization has on the resolving detonation wave properties. A one-dimensional, laminar detonation wave was simulated using the 9-species, 19-step mechanism with various spatial and temporal discretization approaches allowing the wave speed to be compared with the theoretical Chapman-Jouget (CJ) value. The mesh consisted of 1200 hexahedral cells in one spatial dimension with symmetry boundary conditions along the cell sides.

Spatial discretization was calculated using either bounded central differencing (BCD) or second order upwinding (SOU) for momentum, and SOU for pressure, density, species and energy. Temporal discretization was implicit and was either second order bounded or first order. Fig. 4 shows the effect of mesh resolution on detonation wave speed with the CJ speed annotated on the plot. It is clear that both the BCD and SOU spatial discretization significantly overestimate wave speed when used with second order temporal discretization with the disparity increasing as mesh size is decreased. This is a result of an over prediction of peak detonation pressure as there is a strong correlation between wave speed and peak pressure. Switching to first order in time brings the wave speed down significantly, and much closer to the CJ speed and is less dependent on mesh resolution. For reference, the wave speed calculated with an OpenFOAM density-based solver from the University of Michigan known as detFoam [15] is also shown in Fig. 4 which shows similar behavior to the pressure-based solver using the first order temporal scheme.

The effect of acoustic Courant-Friedrichs-Lewy (CFL) number on wave speed is also shown in Fig. 4. For this comparison, CFL number was calculated based on the mesh size and CJ speed. Both the BCD and SOU approaches, when used with the second order temporal approach significantly over predict the wave speed but show improvement as the time step (and CFL) is reduced. The first order temporal scheme slightly under predicts the CJ speed and approaches the CJ speed as the time step is reduced.

The overall conclusion of the one dimensional wave speed simulations is that temporal discretization has a greater influence on predicting wave speed than spatial discretization. The first order temporal scheme is able to predict the correct wave speed and is fairly insensitive to mesh resolution and CFL number, at least for the conditions studied here. It should be pointed out that an accurate simulation of a full three-dimensional RDE with viscous effects using an LES turbulence model requires a numerical approach that can minimize dissipation in the subsonic regions while capturing the detonation wave physics with reasonable accuracy. The compromise chosen here is to use the SOU spatial discretization along with the 2nd order bounded temporal scheme and to maintain the maximum CFL number at 0.4 based on the mesh size and CJ speed which corresponds to an acoustic CFL number of 1.5. The added numerical dissipation of the SOU discretization is enough to keep the predicted wave speed at just 2.5% above the CJ speed for the nominal mesh resolution of 0.5 mm with a modest increase as the mesh is refined. A future study will be needed to assess the effects of the added numerical dissipation on the turbulent fuel-air mixing process.

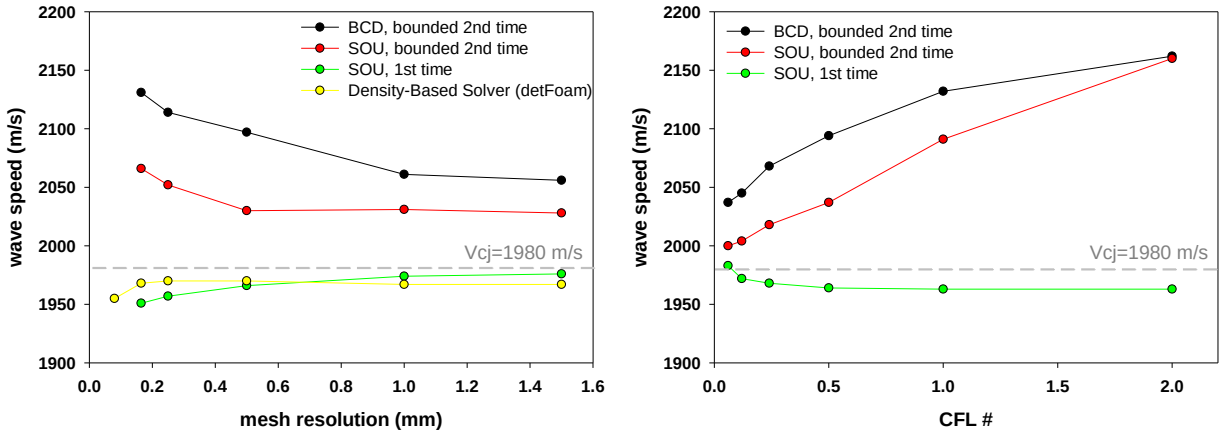

Fig. 4 One-dimensional hydrogen-air detonation simulations. Wave speed vs. mesh resolution (left) and wave speed vs CFL number (right) for a mesh resolution of 0.5 mm.

B. 3-D Modeling

For the 3-D simulations, boundary conditions for the air and fuel inlets were chosen to be constant mass flow inlets and the exit of the annulus was modeled as a pressure outflow. For subsonic outflow regions Fluent imposes the user specified pressure, while for supersonic regions the pressure is interpolated from within the domain. A separate investigation on the effect of the fixed pressure outflow boundary condition was conducted by adding a large plenum onto the exit of the annulus and specifying pressure at the exit of the plenum. Very little difference in terms of wave speed, specific thrust and mean annulus exit pressure was found between the two approaches which is likely due to numerical dissipation minimizing pressure wave reflections from the annulus exit. Specific thrust was calculated by integrating Eq. (5) over the exit plane of the annulus.

$$\frac{1}{\dot{m}}\int[\,V_z\dot{m} + (P\cdot A_e)]dA \tag{5}$$

The walls were modeled as fixed temperature boundaries of 300 K which allows for heat loss to the walls. For the cases presented here the air flowrate was kept fixed at 0.6125 kg/s and the fuel flowrate was kept fixed at 0.01746 kg/s for an equivalence ratio of 1.0, which corresponds to an experimentally studied condition at AFRL [14].

The initialization procedure began with a non-reacting simulation for the entire domain, followed by a separate reacting solution for a truncated domain with premixed fuel and air, which was in turn initialized by patching in a zone of hot, high-pressure products. The premixed solution resulted in a single detonation wave and the pressure and temperature were then patched back into the non-reacting simulation of the entire domain. Limit cycle operation was usually obtained after about 3 to 5 msec of physical time and the solution was then averaged over a period of 1 to 2 msec to derive mean quantities such as static pressure, species concentrations and work-averaged pressure [16].

The 3D results are validated using experimental data consisting of wave speed, number of waves, mean thrust and mean static pressure collected at AFRL [14] as well as wave height and fill zone height measured in an optically accessible RDE [17].

In order to demonstrate the effect the combustion model has on the results, a series of simulations were performed without using any turbulence chemistry interaction (laminar) model followed by series with the same numerical settings but with the PaSR model applied. Fig. 5 shows temperature and pressure contours through the center of the annulus for both simulations with a nominal mesh resolution of 0.5 mm. The laminar model resulted in a two wave solution with an average wave speed of 1790 m/s while the PaSR model resulted in a single wave solution with a wave speed of 1844 m/s and a significantly larger wave height. The higher wave speed for the single wave PaSR mode simulation is consistent with the higher peak pressure which in turn appears to be due to less deflagrative burning ahead of the detonation wave. The experimental data from AFRL show this case to be a single wave result with a wave speed of 1740 m/s. It is believed that the lack of a combustion model over predicts the deflagrative burning in the fill zone which triggers a second detonation wave to form.

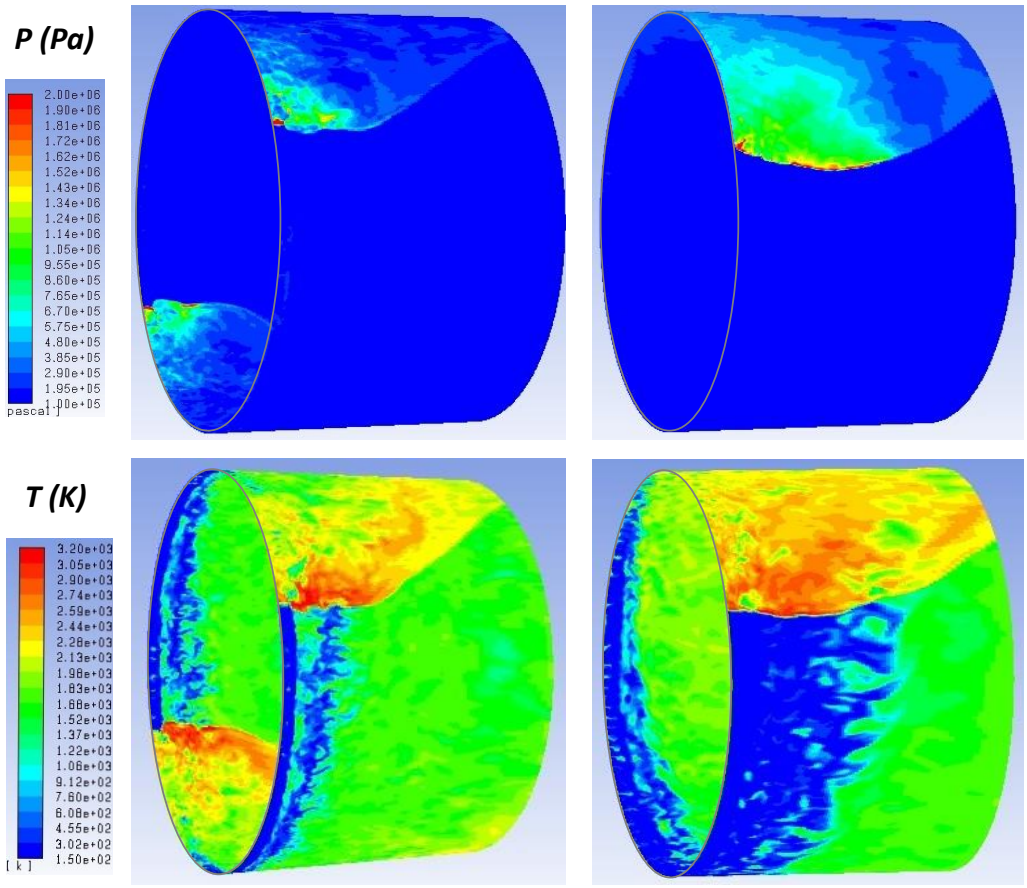

Fig. 5 Pressure contours through center of annulus (top row) for no combustion model (left column) and PaSR model (right column). Corresponding temperature contours in bottom row.

Fig. 6 shows contour plots of temperature, PaSR model constant κ, and the turbulent time scale along the center of the annulus for the nominal mesh size of 0.5 mm. It can clearly be seen how the PaSR model, through the source term modifier, κ affects both the detonation and deflagrative combustion. The average κ in the detonation region was roughly 0.5 and in the deflagrative region it was estimated to be 0.6. There was initially some doubt as to whether the PaSR model would be able to model a stable detonation wave due to the effect that the model constant κ has on the reaction rates. It was found, however that due to the sharp decrease in turbulent mixing time across the detonation wave front (Fig. 6) that the model constant remained large enough (κ ~ 0.5) to sustain the detonation. This may hold true only for the LES modeling approach used here and may be somewhat fortuitous. For a more definitive conclusion, additional work is needed in the area of turbulence interaction with detonation waves.

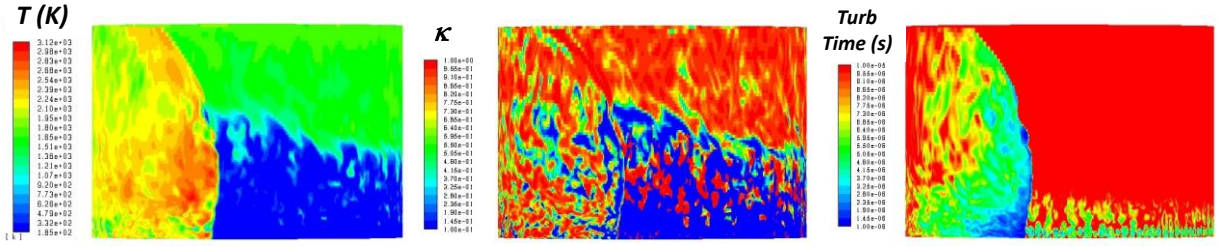

Fig. 6 Contours of temperature (left), PaSR model constant κ (middle), and turbulent time scale (right) for nominal mesh resolution of 0.5mm

Two contour plots of the $\log_{10}$ of the volumetric heat release for the baseline mesh size of 0.5 mm with the laminar and PaSR models are shown in Fig. 7. The PaSR model data is the same as in Fig. 6. The logarithmic scale shows five orders of magnitude of heat release and demonstrates the significant effect that the PaSR model has on combustion in the contact layer and fill zone ahead of the detonation wave. Note that the laminar model solution contained two detonation waves with only one shown in Fig. 7. The increased deflagrative burning ahead of the detonation wave, often referred to as parasitic combustion seems to spawn additional detonation waves and thus reduces the detonation wave height.

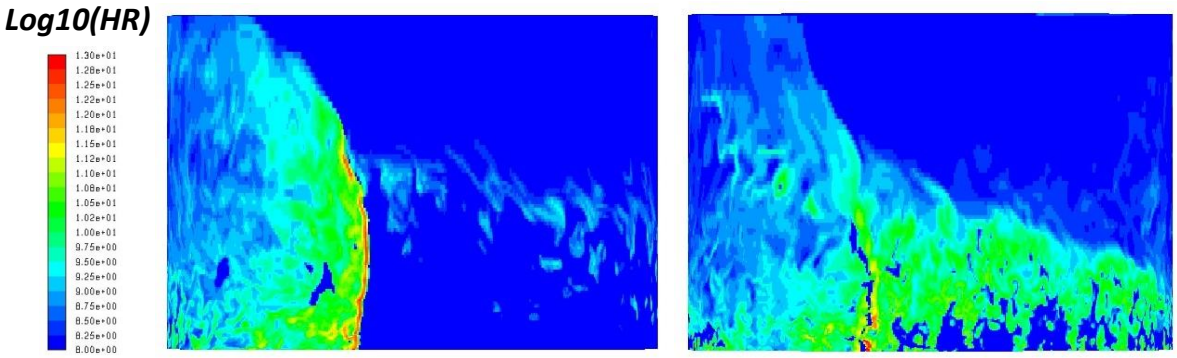

Fig. 7 Contours of $\log_{10}$ of the volumetric heat release through the center of annulus with PaSR model (left), and laminar model (no turbulence chemistry interaction, right) for a nominal mesh resolution of 0.5mm.

Combustion occurring by deflagration represents a loss in potential work due to the higher entropy production compared to detonative burning. An accurate assessment of the percentage of heat release in each mode is not trivial. A rough estimation using a pressure of 20 atm as a cutoff for delineating between detonation and deflagration indicates that about half of the heat release occurs in the detonation wave. Fig. 8 shows the heat release distributions in the form of histograms of fractional heat release verses static pressure for both the laminar and PaSR simulations on the base mesh size of 0.5 mm. Since the bins represent fractional heat release, the sum of the bins for any case always sums to one.

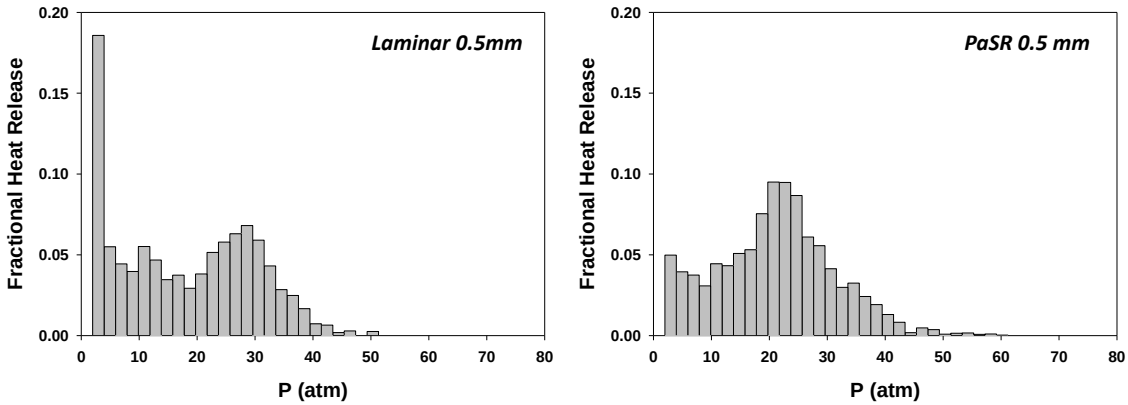

Fig. 8 Distribution of fractional heat release as a function of pressure for the laminar simulation (left) and the PaSR simulation (right) for the baseline mesh size of 0.5mm.

C. Mesh Resolution Study

The effect of mesh size on the results was studied by refining as well as coarsening the baseline 0.5 mm mesh. The finest mesh was created by adapting the 0.5 mm mesh in the detonation region resulting in a mesh size of 0.25 mm in the detonation zone and an overall mesh count of 29 million cells. The coarser meshes were created independently from the baseline within the Gambit mesher and range from 0.75 to 1.5 mm in the detonation zone with mesh counts spanning from 2 million to 0.6 million cells, respectively.

Fig. 9 shows a series of contour plots of static temperature versus mesh resolution for both the "laminar" combustion model, which ignores turbulence chemistry interaction, and the PaSR model. Several key differences can be observed between the two combustion modeling approaches. With the laminar approach, multiple detonation waves form and the number of waves changes from three to two as the mesh is refined. At the finest resolution of 0.25 mm, the detonation waves collapse and the combustion is dominated by deflagration. This is likely due to the over-prediction of heat release in the absence of a combustion model. The series of simulations with the PaSR model show a single wave solution for all resolutions studied which is consistent with the experimentally observed single wave for this condition.

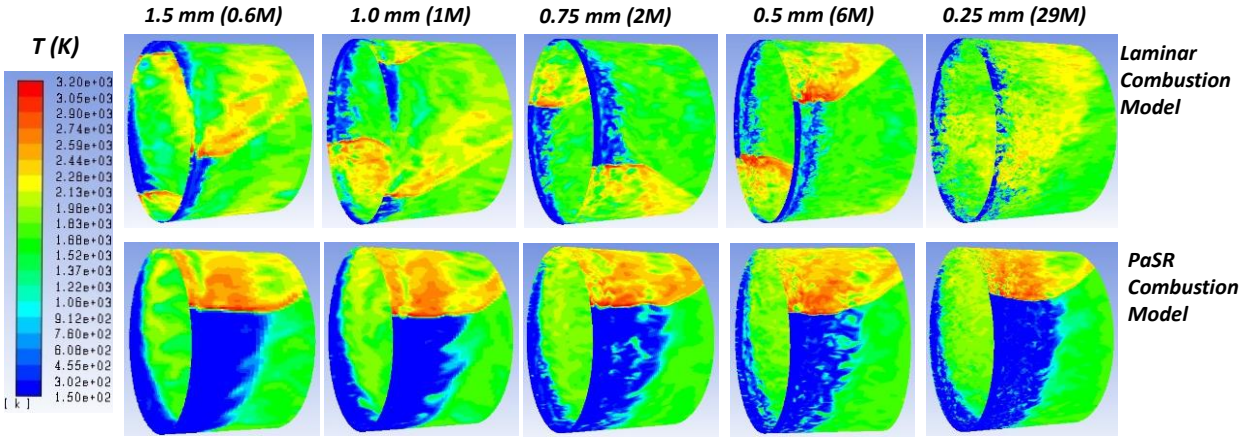

Fig. 9 Contours of temperature for "laminar" combustion model (top row) and PaSR model (bottom row). Mesh resolution refined from 1.5 mm to 0.25 mm (left to right).

Wave speed was characterized by probing a single point in the detonation region and averaging the wave transit time over multiple detonation cycles. Peak detonation pressure was calculated by monitoring the peak cell pressure in the detonation region and averaging in time. A plot of both parameters as a function of mesh resolution is provided in Fig. 10. The wave speed correlates well with peak pressure for mesh sizes larger than 0.5 mm but while peak pressure continues to increase for the finer mesh sizes, the wave speed begins to decrease. The experimentally measured wave speed for this condition was 1740 m/s which is substantially less than the CFD predictions (1850 to 1950 m/s). The 1D analysis shown in Fig. 4 depicts a wave speed that increases with decreasing mesh size which is consistent with the 3D results shown in Fig. 10 for mesh sizes larger than 0.5mm.

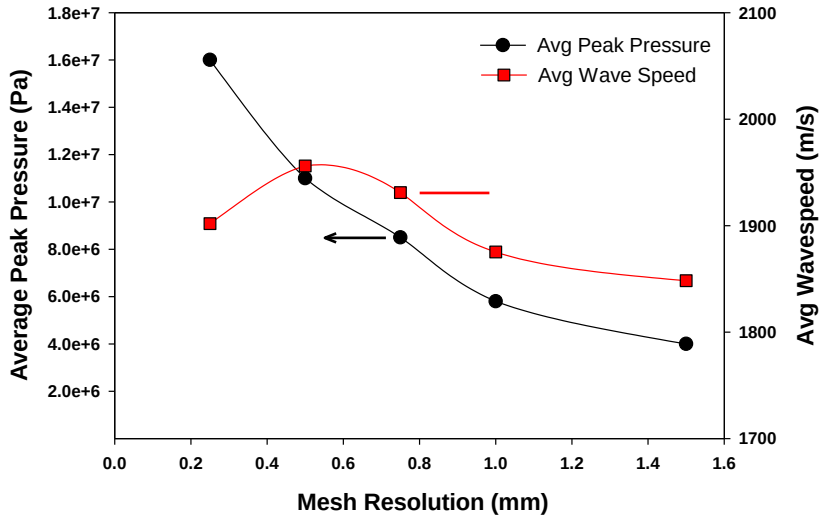

Fig. 10 Average peak pressure in the detonation wave and average wave speed as a function of mesh resolution with the PaSR model.

Further analysis of what could be affecting wave speed for the mesh sizes studied here was conducted by analyzing the unburned mixture properties just ahead of the detonation wave. A 20 degree sector of the unburned gasses in the fill region just ahead of the detonation wave revealed a complex effect of mesh resolution on the results. Fig. 11 is a plot of fill zone pressure along with the mean and rms mixture fraction of hydrogen atoms. Mixture fraction, which is typically used in lieu of equivalence ratio for non-premixed combustion, is defined as the total mass fraction of hydrogen atoms and is equal to 0.0285 at stoichiometric conditions for hydrogen-air combustion.

The mean mixture fraction in the fill zone was found to increase from 0.026 to 0.035 (corresponding to an equivalnce ratio increase from 0.9 to 1.22) as the mesh is refined from 1.5 mm to 0.25 mm. This is believed to be due to the effect of mesh resolution on manifold dynamics and injector recovery. As peak pressure increases with decreasing mesh size, the air manifold is impacted to a greater extent than the fuel manifold behind the detonation wave due to the lower injector pressure differential on the air side. This in turn creates an increasingly fuel rich region ahead of the detonation wave as mesh size is reduced. Calculations of the CJ speed show that V_{CJ} increases from 1934 to 2044 as mixture fraction is increased form 0.026 to 0.035. This 110 m/s increase in theoretical wave speed is close to the 100 m/s increase oberved in Fig. 10 between 1.5 mm and 0.5 mm mesh resolution.

One explanation for the rolloff in wave speed at the finest mesh resolution is the effect that fuel-air unmixedness, as measured by rms mixture fraction shown in Fig. 11, has on wave speed. The decrease in rms mixture fraction as mesh size is increased is due to the increased numerical dissipation of the coarser mesh, which in turn artifically improves fuel-air mixing. This artifically improved mixing likely increases the wave speed. As mesh size is reduced, there is a competition between increasing wave speed due to the increase in mean mixture fraction, and the effect of fuel-air mixing as shown in Fig. 11. It is possible that the mesh resolution of 0.5 mm represents an inflection point where unmixedness begins to affect wave speed more than the mean mixture fraction does. Note that there is also a purely numerical effect of mesh resolution on wave speed, which is due to the reduced numerical dissipation increasing the peak pressure, and thus wave speed, as observed in Fig. 4.

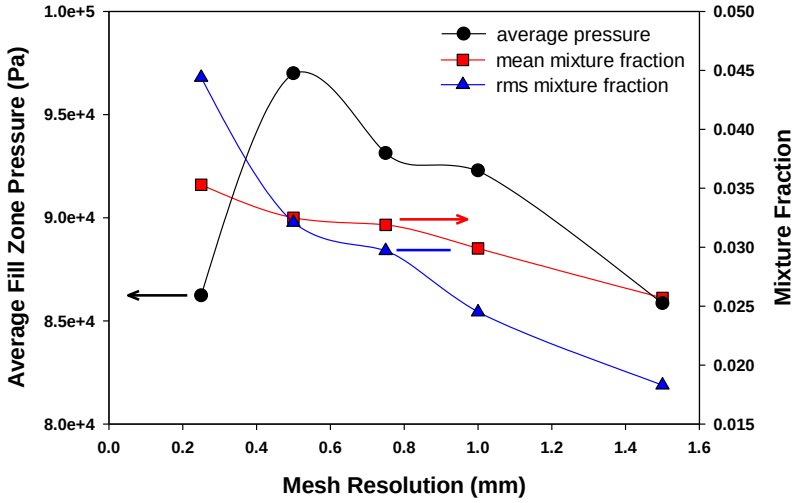

Fig. 11 Average fill zone pressure, mean mixture fraction and rms mixture fraction vs. mesh resolution for the PaSR simulations. Fill zone defined as unburned gases in a 20° sector ahead of the detonation wave.

The fill zone pressure follows a similar pattern to the wave speed but it is not clear if this is a cause or effect. Calculations of V_{CJ} show an increase of just 4 m/s over the range of fill zone pressures oberved. Factors such as viscous pressure drop along the walls of the combustor could play a more prominent role in fill zone pressure as the mesh resolution is changed. Also, mesh resolution may impact deflagrative burning which could play a role in fill zone pressure through expansion of the hot combusiton products. Fill zone axial veloxity does seem to follow an inverse trend with respect to fill zone pressure. As the fill zone pressure decreases, there is a corresponding increase in axial velocity.

The specific thrust derived from the CFD simulations was insensitive to mesh resolution and was roughly 1075 N while the experimentally measured specific thrust was 836 N [14]. Over prediction of thrust seems to be a common discrepancy observed between CFD and experimental measurements on a variety of geometries, propellants and CFD codes. Additional study is required to clearly determine the source of this discrepancy.

Plots of fractional heat release as a function of pressure are presented in Fig. 12. As was done for the analysis shown in Fig. 8, the combustor pressure is grouped into 40 bins ranging from zero to 80 atm. The amount of heat release in each bin is summed and normalized by the total heat release and plotted in Fig. 12. The plots do seem to show an increase in heat release at the highest pressures (as indicated by the tail in the distribution in Fig. 12) as the mesh is refined. There also seems to be an increase in heat release at the lowest pressures as the mesh is refined. An analysis of detonative combustion, defined as the fraction of heat release at pressures above 20 atm, results in a detonative fraction between 56% and 61% for the five simulations. This seems to indicate that the fraction of detonative combustion using this type of coarse data analysis is fairly insensitive to mesh size even though there is some change in the distribution of heat release as the mesh is refined.

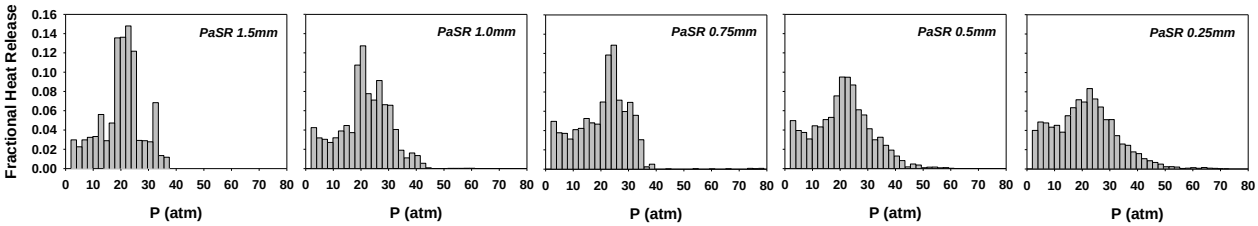

Fig. 12 Distribution of fractional heat release as a function of pressure for the five mesh resolutions studied using the PaSR model. Mesh size decreasing from left to right.

The last validation exercise was conducted with measurements of detonation wave height and fill zone height measured with infrared (IR) imaging in an optically accessible RDE [17]. This version of the AFRL RDE was of the same geometry studied here with the only difference being the use of a quartz outer-body. The IR camera measured black body radiation of water at 2.89um permitting a comparison to be made with the CFD simulation data using a comparable parameter of water concentration multiplied by temperature to the fourth power. The experimental detonation wave height was determined by the distance from the injection plane to the axial location where the IR emission decreased to 50% of the peak value within the detonation wave front measured with phase averaged images. The fill zone height was measured as the distance from the injection plane to the threshold of IR emission just ahead of the detonation wave. A similar process was used in the analysis of the CFD simulations with the notable difference being that the experimental IR data is line of sight integrated while the CFD results are simply take along the center of the annulus averaged over several instances in time. Fig. 13 shows the detonation wave height and fill zone height as a function of mesh resolution along with the experimental values shown with dashed lines. The overall agreement with the experimental data is fairly good for mesh resolutions finer than 1 mm. The increase in both detonation wave height and fill zone height could be affected by the fill zone pressure as shown in Fig. 11. As the fill zone pressure decreases, the fill zone axial velocity increases thus increasing the detonation wave height. Some effect from the wave speed may also play a role in wave height.

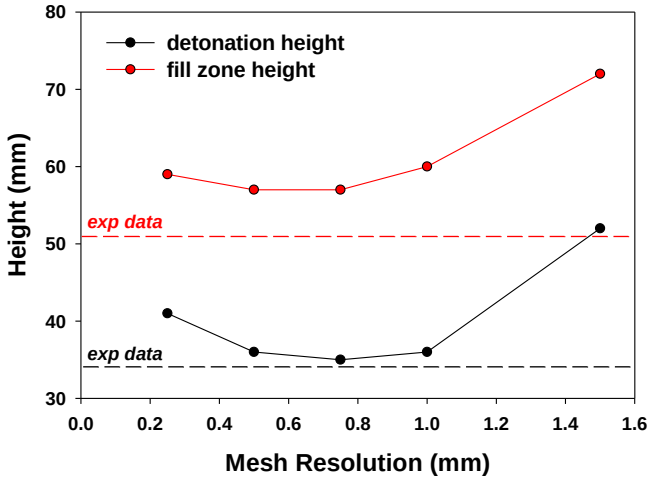

Fig. 13 Detonation wave height and fill zone height vs. mesh resolution. Experimental values annotated with dashed lines.

V. Conclusions and Future Work

Simulations of a hydrogen-air RDE with detailed chemistry and ignoring turbulence chemistry interactions was found to predict more detonation waves than experimentally observed. Use of a simple, zero-dimensional PaSR model based on modification of the chemical source terms using a ratio of turbulent mixing time to chemical reaction time was found to predict the correct number of detonation waves (one wave for the case studied here).

The conclusions of the mesh resolution study are that a mesh independent solution was achievable in terms of the number of waves and the specific thrust, but not in terms of wave speed or the mixture properties of the fill zone. A further decrease in mesh size would need to be conducted to see if a fully mesh independent solution could be achieved. The fact that even at the finest resolution the wave speed (1902 m/s) was significantly higher than the experimental wave speed (1740 m/s) is indicative of the limitations of the implicit pressure-based approach used here and is consistent with the findings of the 1-D wave speed studies.

Reducing the mesh size did have an effect on fuel-air mixing in the fill zone by reducing numerical dissipation which in turn reduced mixing and thus wave speed. This effect was somewhat offset by the increasing mean mixture fraction in the fill zone which is believed to be due to changes in manifold and injector dynamics as the peak detonation pressure increased with decreasing mesh size. The variation of pressure in the fill zone with mesh resolution has only a minor effect on wave speed but deserves further investigation to determine if this is a cause or effect.

Specific thrust was mostly independent of mesh resolution and while the heat release distribution with respect to pressure does show some dependency on mesh resolution the overall fraction of heat release due to detonation verses total heat release was relatively constant and in the range of 56% to 61%.

Lastly, the detonation wave height and fill zone height derived from the CFD simulations showed good agreement with the experimental data for mesh resolutions finer than 1.0 mm. Some effect of mesh resolution at the finest mesh size was observed and may be attributed to a decrease in fill zone pressure. Future studies will look further into the effects of mesh resolution on fill zone properties.

Acknowledgments

This work was performed in support of the US Department of Energy's Fossil Energy Advanced Turbines Research Program. The authors would like to thank the support of the DoE Advanced Turbines Program and Technology Manager Mr. Richard Dennis.

Disclaimer

References

[1] Schwer, Douglas and Kailasanath, Kailas, "Numerical Investigation of the Physics of Rotating-Detonation-Engines", Proceedings of the Combustion Institute, 33, 2011, 2195-2202.

[2] Schwer, Douglas and Kailasanath, Kailas, "Numerical Study of the Effect of Engine Size on Rotating Detonation Engines", AIAA 2011-581, 49th AIAA Aerospace Sciences Meeting, Jan. 4-7, 2011, Orlando, FL.

[3] Theoretical and Numerical Combustion, 2nd Edition, Thierry Poinsot and Denis Veynante, R.T. Edwards Pubs., 2005.

[4] D. Veynante and L. Vervisch, "Turbulent Combustion Modeling", Prog. Eng. Comb. Sci., Vol. 28, 2002, pp. 193-226.

[5] Chomiak J.and Karlssom, A. "Flame Liftoff in Diesel Sprays", 26th Symposium (International) on Combustion, The Combustion Institute, pp. 2557-2564, 1996.

[6] Chomiak J. "Combustion: a study in theory, fact and application" Abacus Press/Gorden and Breach Science Publishers; 1990.

[7] P. Givi, "Filtered Density Function for Subgrid Scale Modeling of Turbulent Combustion", AIAA J., Vol. 44 (1), 2006, pp. 16-23.

[8] Marco Ferrarotti, Zhiyi Li and Alessandro Parente, "On the Role of Mixing Models in the Simulations of MILD Combustion Using Finite-Rate Chemistry Combustion Models", Proc. Comb. Inst., 37, 4531-4538, 2019.

[9] Zhiyi Li Marco Ferrarotti, Alberto Cuoci and Alessandro Parente, "Finite-ate Chemistry Modeling on Non-Conventional Combustion Regimes Usign a Partially-Stirred Reactor Closure: Combustion Model Formulation and Implementation Details", Applied Energy, 225, 637-655, 2018.
[10] Byggstøyl, S. and Magnussen, B. F., *Turbulent Shear Flows 4*, Springer Verlag, Berlin, 1985, pp. 381–395.
[11] Bjorn F. Magnussen, "On the Structure of Turbulence and a Generalized Eddy Dissipation Concept for Chemical Reaction in Turbulent Flow", Presented at the 19th AIAA Aerospace Sciences Meeting, St. Louis, Missouri, Jan. 12-15, 1981.
[12] K.R.V. Manikantachari, Scott Martin, Ramees K. Rahman, Carlos Velez and Subith Vasu, "A General Study of Counterflow Diffusion Flames for Supercritical CO2 Mixtures", GT2019-90332, Proceedings of ASME Turbo Expo, June 17-21, 2019, Phoenix, Arizona.
[13] Li, J., Zhao, Z., Kazakov, K., and Dryer, F., 2004, "An Updated Comprehensive Kinetic Model of Hydrogen Combustion," Int. J. Chem. Kinet., **36**_10_, pp. 566–575.
[14] Rankin, Brent A., Fotia, Matthew, L., Paxson, Daniel E., Hoke, John L. and Schauer, Frederick R., "Experimental and Numerical Evaluation of Pressure Gain Combustion in a Rotating Detonation Engine", AIAA 2015-0877, 53rd AIAA Aerospace Sciences Meeting, Jan. 5-9, 2015, Kissimmee, FL.
[15] Takuma Sato and Venkat Raman, "Analysis of Detonation Structures with Hydrocarbon Fuels for Application Towards Rotating Detonation Engines", AIAA Propulsion and Energy Forum Joint Propulsion Conference, July 9-11, 2018, Cincinnati, OH.
[16] Strakey, P., Ferguson, D., Sisler, A., Nix, A, "Computationally Quantifying Loss Mechanisms in a Rotating Detonation Engine", 54th AIAA Aerospace Sciences Meeting, San Diego, CA, 2016.
[17] Brent A. Rankin, Joshua C. Codoni, Kevin Y. Cho, John L. Hoke and Frederick R. Schauer, "Investigation of the Structure of Detonation Waves in a Non-Premixed Hydrogen-Air Rotating Detonation Engine Using mid-Infrared Imaging", Proc. Comb. Inst., 37, 2019, 3479-3486.